Journal of Power Sources 213 (2012) 350–357

Contents lists available at SciVerse ScienceDirect

Journal of Power Sources

journal homepage: www.elsevier.com/locate/jpowsour

Shape-alterable and -recoverable graphene/polyurethane bi-layered composite film for supercapacitor electrode

Zhixin Tai [a,b], Xingbin Yan [a,*], Qunji Xue [a]

[a] State Key Laboratory of Solid Lubrication, Lanzhou Institute of Chemical Physics, Chinese Academy of Science, 18#, Tianshui Mid Road, Lanzhou 730000, China
[b] Graduate University of Chinese Academy of Sciences, Beijing 100080, China

ARTICLE INFO

Article history:
Received 13 January 2012
Received in revised form
13 March 2012
Accepted 15 March 2012
Available online 26 April 2012

Keywords:
Graphene paper
Shape-memory polyurethane
Composite
Supercapacitor

ABSTRACT

In this paper, a graphene/shape-memory polyurethane (PU) composite film, used for a supercapacitor electrode, is fabricated by a simple bonding method. In the composite, formerly prepared graphene paper is closely bonded on the surface of the PU slice, forming a bi-layered composite film. Based on the good flexibility of graphene paper and the outstanding shape holding capacity of PU phase, the resulting composite film can be changed into various shapes. Also, the composite film shows excellent shape recovery ability. The graphene/PU composite film used as the electrode maintains a satisfactory electrochemical capacitance of graphene material and there is no decay in the specific capacitance after long-cycle testing, making it attractive for novel supercapacitors with special shapes and shape-memory ability.

1. Introduction

Nowadays, with the development of the electronic devices, the current energy-storage devices including different batteries and capacitors need much more attention in order to meet the rapid growing demand of the modern market. Among them, supercapacitors, exhibiting energy density higher by orders of magnitude than conventional capacitors, and greater power density and longer cycling life than common batteries, have attracted considerable attention [1]. Up to now, transition metal oxides, conducting polymers and various carbon materials have been used as supercapacitor electrode materials [2–5]. On the other hand, in order to adapt to the wide circumstance, one of the research trends of supercapacitors is developing small, thin, lightweight, and flexible electrode materials [6]. So conceivably, developing special shaped supercapacitor electrodes with maintaining the high specific capacitance could further expand the field of application of supercapacitors.

Graphene nanosheets (GNSs), as a new class of two-dimensional carbon nanostructure material, have attracted much attention from both the experimental and theoretical research communities in recent years [7–9]. Up to date, many approaches have been developed to prepare graphene materials. Also, similar to carbon nanotubes, graphene oxide (GO) sheets and GNSs can indeed be assembled into paper-like materials [10–13]. Such free-standing, paper-like GO and graphene materials have displayed excellent flexibility and mechanical stiffness combined with exceptional electrical conductivity (for graphene paper) [14,15]. And hence it makes them potentially suitable for flexible electrochemically active materials, such as fuel cells, electrical batteries and supercapacitors [16]. For example, Lee et al. reported that the specific capacitance of graphene paper is 141.5 F g^{-1} at the current density of 0.5 F g^{-1} [17]. Moreover, Wu et al. prepared paper-like graphene/polyaniline nanofiber composite films of by vacuum filtration and showed that the composite films possess high capacitance and excellent cycling stability [18].

As we know, supercapacitors are constructed much like a battery in that there are two electrodes immersed in an electrolyte, with an ion permeable separator located between the electrodes [19]. Because the graphene paper can be bent and even rolled-up, it would be benefited for the preparation of special shape supercapacitor electrodes. However, the bent shape of graphene paper can't be kept forever if there is no assistant material.

Thermal-responsive shape-memory polymers (SMPs), a class of intelligent materials that can be fixed at a temporary shape below their transition temperature and thermally triggered to resume their original shapes on demand, hold great potential as self-fitting scaffolds or implants, tunable encapsulating materials and grafting materials [20]. The intrinsic mechanism for shape-memory behavior of polymers is the freezing and activation of the long-range

* Corresponding author. Tel./fax: +86 931 4968055.
E-mail address: xbyan@licp.cas.cn (X. Yan).

0378-7753/$ – see front matter © 2012 Elsevier B.V. All rights reserved.
doi:10.1016/j.jpowsour.2012.03.086

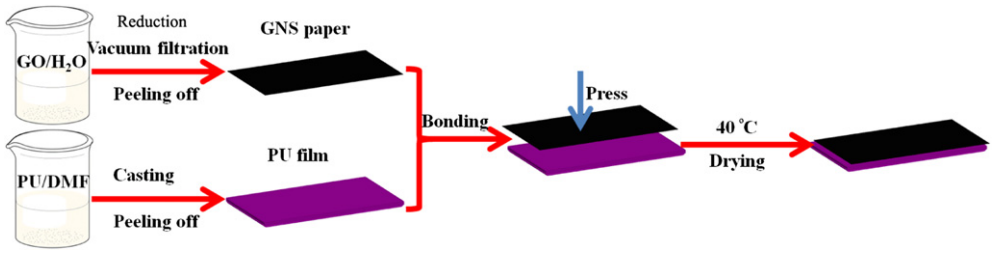

Scheme 1. The preparation procedure of the graphene/PU composite film (black—graphene paper, yellow—PU film). (For interpretation of the references to color in this figure legend, the reader is referred to the web version of this article.)

motion of polymer chain segments below and above transition temperature, respectively. As one member of the SMPs, shape-memory polyurethane (SMPU), by introducing special functionalized soft segment (SS) and hard segment (HS) into the polymers, can be deformed and the temporary shape can be fixed at room temperature, yet the original shape can still be recovered at an elevated temperature [21,22]. Therefore, it is expected that, SMPU would be a good choice to be used as the assistant material for the preparation of special shaped graphene paper electrodes. In addition, polymer can also be as a kind of encapsulation for supercapacitors [6].

There is currently a strong demand for flexible energy-storage devices, based on batteries and supercapacitors, to meet the various requirements of modern gadgets [23–27]. First, the electrochemical capacitor with the shape-memory function can be used under different conditions, especially that the conventional electrochemical capacitor with the shape of the traditional (rectangle, cylinder, etc.) can't be fixed when the space is limited. The second, the shape-memory graphene/polyurethane composite film, characterized by their lightweight and flexibility, is promising for producing wearable or rolling-up electrodes [28,29]. The third, polymer can also be direct as a kind of encapsulation for supercapacitors [6]. Therefore, the shape-memory graphene/polyurethane composite film would be a promising material in the potential energy-storage applications.

In this study, a novel bi-layered graphene/SMPU composite film was prepared via a simple bonding method. The graphene/SMPU composite film can be made into different shapes and shows excellent shape fixity and recovery behavior. Moreover, its microstructure and electrochemical properties were investigated, respectively. As results, the layer-by-layer structure and the electrochemical capacitance of graphene paper are both retained in the composite film. This graphene/SMPU composite will be useful for the development of next-generations of tunable electrode materials.

2. Experimental

2.1. Materials

High-purity (99.99%) graphite (325 mesh) was used to prepare GO. ε-caprolactone (CL) and 4,40-methylenediphenyl diiso-cyanate (MDI) were received from Acros. N,N-dimethylformamide (DMF, 99%), 1,4-butanediol (BDO), 4-nitroaniline, stannous octoate, ethylene glycol and dibutyltin dilaurate (DBTDL) were bought from Tianjin Reagent Co. Ltd., China. Before use, 4-nitroaniline, ethylene glycol, BDO, DBTDL, CL and DMF were dried with CaH_2 for 24 h and freshly distillated.

2.2. The preparation of graphene paper

2.2.1. Preparation of GO

Graphite oxide was synthesized from natural graphite by a modified Hummers' method as originally presented paper [30,31]. In a typical synthesis, graphite powder (3 g) was put into a solution of concentrated H_2SO_4 (12 mL), $K_2S_2O_8$ (2.5 g), and P_2O_5 (2.5 g). The mixture was kept at 80 °C for 4.5 h using a hotplate. Successively, the mixture was cooled to room temperature (RT) and diluted with 0.5 L of H_2O and left overnight. Then, the mixture was filtered and washed with H_2O using a 0.45 μm millipore-filter to remove the residual acid. The product was dried under ambient condition. This pre-oxidized graphite was then subjected to oxidation by Hummers' method described as we reported [32].

2.2.2. Preparation of graphene paper

Graphene paper was prepared in according to the literature [33]. Typically, the as-prepared graphite oxide was dispersed in water to create a 0.05 wt% dispersion. Exfoliation of graphite oxide to GO was achieved by ultrasonication of the dispersion at 500 W for 30 min. The obtained brown dispersion was then subjected to 30 min of centrifugation at 3500 rpm to remove any un-exfoliated graphite oxide. In a typical procedure for chemical reduction of GO to graphene, the resulting homogeneous dispersion was mixed with some water to the 50 ml in a 250 ml three-neck flask. After being stirred and fed N_2 for 60 min, 25.0 μl of hydrazine solution and 175.0 μl of

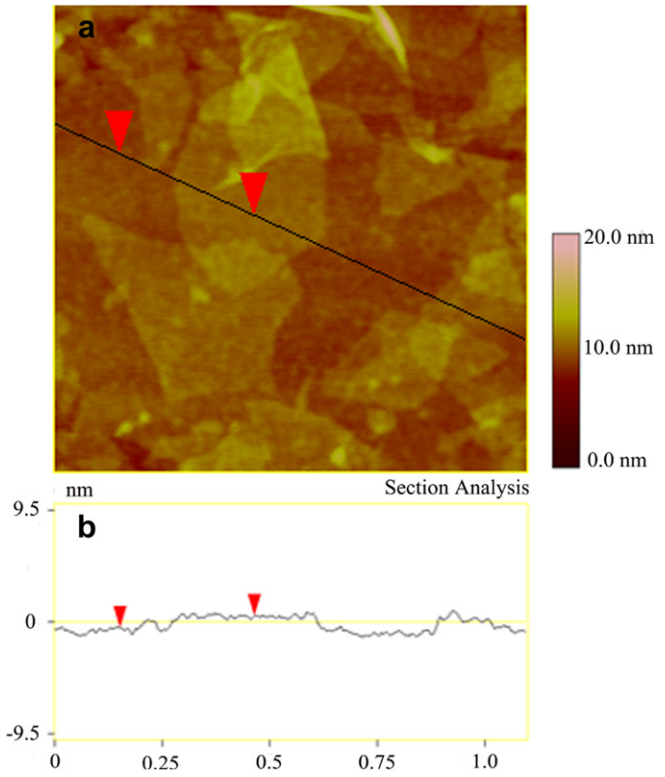

Fig. 1. The morphology of GNSs: (a) AFM image of GNSs and (b) the height analysis of an individual GNS.

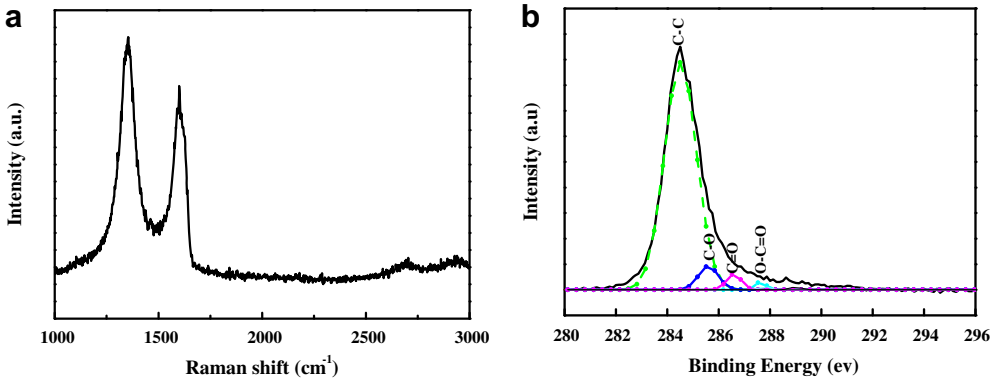

Fig. 2. The Raman (a) and XPS (b) spectra of GNSs.

ammonia solution (28 wt% in water) were put in the flask. Then, the mixture was heated to the 95 °C and kept for 2 h. At last, the resulting mixture was filtered using a 0.45 μm millipore-filter and washed with H_2O to remove the residual impurities. The filter coated with GNSs was dried under ambient condition and the graphene paper was obtained by peeling off from the filter finally.

2.3. Preparation of polycaprolactone/polyurethane (PCL/PU)

2.3.1. Preparation of polycaprolactone diols (PCL-diols)

A certain amount of ε-CL and ethylene glycol with a stoichiometric ratio were mixed in a flask, and then 0.05 wt% stannous octoate was added as catalyst. The reaction was carried out under pure nitrogen at 130 °C for 24 h. The polymer was precipitated in cold diethyl ether and then deterged by methanol. Then the product was dried at 30 °C in vacuum.

2.3.2. Preparation of PCL/PU

First, MDI and PCL-diols were dissolved in DMF in a dry three-necked flask. The mixture was stirred under nitrogen at 80 °C for 2 h to prepare the polymer precursor. Second, the BDO chain extenders were subsequently added, and then the mixture was kept at 80 °C for 3 h to fulfill the polymerization. DMF was added gradually during the extender reaction to avoid too sticky. At last, solid content of mixture was about 20–30%.

2.3.3. Preparation of the GNS/PU composite film

Scheme 1 shows the preparation steps of the bi-layered graphene/PU composite film. In detail, fresh prepared PCL/PU solution was casted on a Teflon plate and dried at 80 °C for 24 h to evaporate most of DMF. The film sample coated on Teflon was further dried in a vacuum oven at 80 °C for another 24 h and then the film was peeled off from the Teflon plate to obtain a free-standing PU film with a thickness of 2–3 mm. The prior-prepared graphene paper was immersed into DMF solvent for 10 min. After that, the wet graphene paper was bonded with the PU film. After being dried in the vacuum oven at 80 °C for 24 h, a graphene/PU composite film was obtained and it could be cut into rectangle shape with an area of 10 mm × 20 mm.

2.4. Characterization

The fracture surface morphology of as-prepared composite film and the top-morphology of graphene layer were characterized using a high-resolution scanning electron microscope (HR-SEM, JSM-6701). The microstructure of graphene sample was investigated by a Lab RAMHR800 Raman spectroscopy (Horiba, Hobin Yvon, France, at 532 nm laser excitation). In order to analyze species of the GNSs, the chemical bonding states were identified on a Perkin–Elmer PHI-5702 multi-functional X-ray photoelectron spectroscopy (Physical Electronics, USA), using Al-Kα radiation (photon energy 1476.6 eV) as the excitation source and the binding energy of Au (Au $4f_{7/2}$: 84.00 eV) as the reference. The thickness of GNSs was estimated using a atomic force microscope (Nanoscope III, Digital Instruments Co.) in tapping mode using a Si base under ambient conditions with a scanning rate of 1 Hz. Fourier transform infrared (FTIR) spectrum of as-prepared PCL/PU was measured using an IR Spectrophotometer (Bruker IFS 66v s^{-1}, German) within a range of 4000–400 cm^{-1}.

2.5. Electrochemical measurements of the graphene/PU composite paper

The electrochemical properties of the film samples were carried out using an electrochemical working station (CHI660D, Shanghai, China) in a conventional Teflon electrochemistry cell with a three-electrode system in 1 M H_2SO_4 electrolyte at the room temperature: a working electrode (WE, GNS/PU film), a platinum wire counter electrode and a saturated calomel reference electrode.

The cyclic voltammetry (CV) curves were collected with a potential window from 0 V to 0.8 V *versus* SCE at different scan rate from 5 to 100 mV s^{-1}. Electrochemical impedance spectroscopy (EIS) measurements were recorded from 100 kHz to 100 mHz at the open circuit potential. Galvanostatic charge/discharge measurements were run on from 0 V to 0.8 V at different current density. The weight of the graphene paper was 4 mg. The cycling stability test

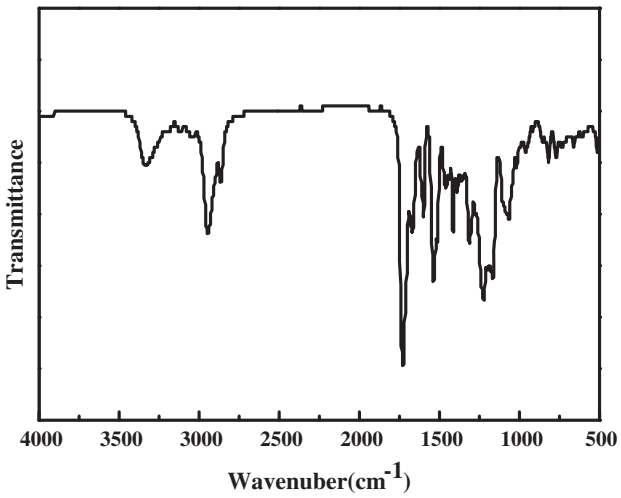

Fig. 3. FTIR spectrum of as-prepared PCL/PU.

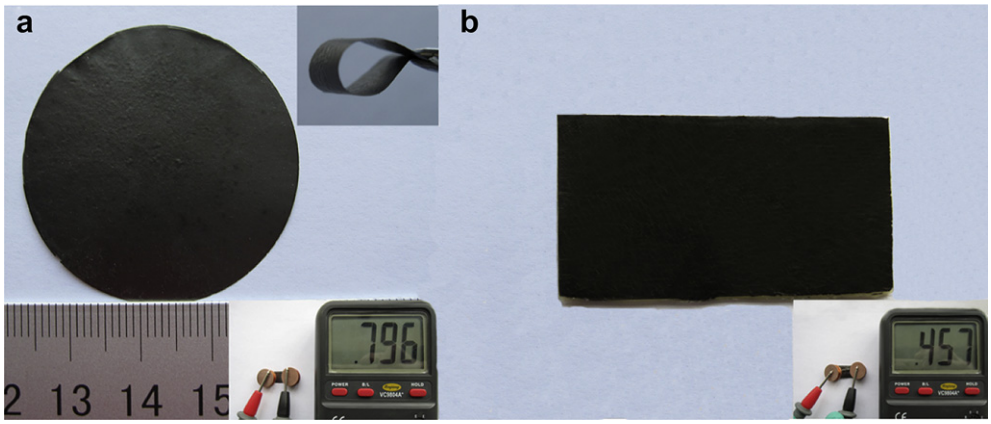

Fig. 4. Digital camera images of the samples. (a) A piece of graphene paper. A graphene paper (top-right inset) is bent to demonstrate its flexibility. The value of ohmmeter (bottom-right inset) is about 800 Ω. (b) As-prepared graphene/PU composite film. The value of ohmmeter (bottom-right inset) is about 460 Ω. It may result from the enhancing contact among the GNSs after the pressing during the preparation procedure of the graphene/PU composite film.

was evaluated with a Land CT2001A battery program-control test system (LAND, Wuhan, China). The capacitance is calculated from the slope of the discharge curve, according to the equation

$$C = (I \times \Delta t)/(\Delta V \times m)$$

where C is the specific capacitance, I is the constant discharge current ($A\,g^{-1}$), Δt is the discharge time (s), ΔV is the voltage window in discharge curve (V) and m is the mass of the working electrode (g).

3. Result and discussion

As shown in Fig. 1, the AFM image and the corresponding height profiles show that GNSs on a single-crystal silicon surface are thin with an average thickness of 1.0 nm, which is larger than the corresponding value of ideal single-layered GNSs (0.34 nm). It is owing to that a small number of oxygen-containing groups still remain on the surfaces of GNSs [33].

Fig. 2(a) shows a typical Raman spectrum of as-prepared GNSs, which is a fast and non-destructive method for the characterization of carbons. The G peak (1580 cm^{-1}), D peak (1360 cm^{-1}) and 2D peak (2700 cm^{-1}) are clearly visible in the curve, which demonstrate that GNS is a typical carbon structure. Also, the relatively high intensity ratio between D peak and G peak indicates the realization of deoxygenation in chemically reduced GNSs.

As shown in Fig. 2(b), XPS measurements are performed to confirm the chemical composition of the GNSs. The C1s XPS spectrum of GNSs after the Gaussian fitting indicates the presence of four types of carbon bonds: C–C (284.5 eV), C–O (286.6 eV), C=O (287.8 eV) and O–C=O (289.0 eV). Though these oxygen-containing functionalities show much smaller intensities compared with C–C bond, their presence indicates the chemical reduction with hydrazine hydrate is not thorough and a small quantity of oxygen functional groups still retain on GNSs. These activated groups would provide an additional pseudo-capacitance contribution to the graphene supercapacitors [1].

FTIR spectroscopy is widely used for identification of polymers because of its sensitivity to minor variations in polymer structure. Fig. 3 shows the FTIR spectrum of as-prepared PU polymer. The absorption peak of at 3315 cm^{-1} indicates the N–H stretch in carbamate. The peaks at 2980–2850 cm^{-1} are associated to C–H stretch of CH_3, CH_2 and CH. The characteristic absorption peaks at

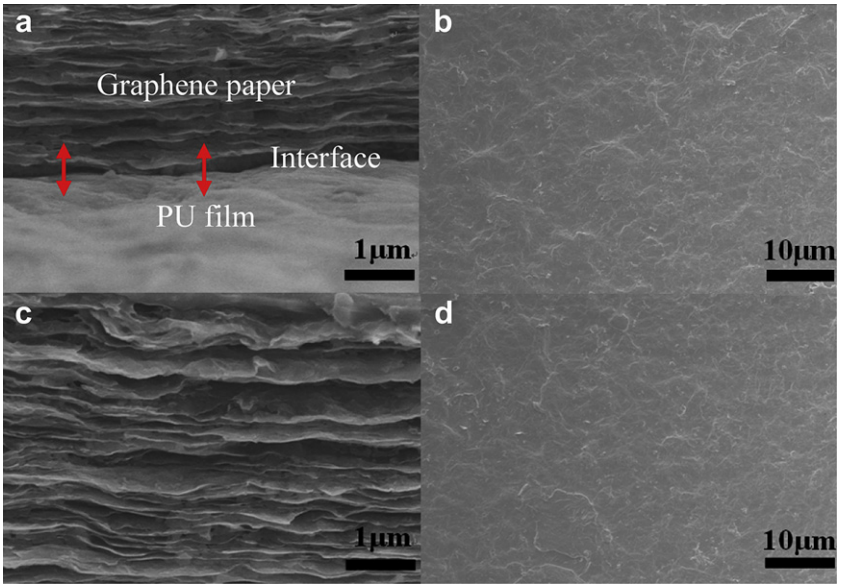

Fig. 5. SEM images of the graphene paper and the graphene/PU composite film: (a and c) the fracture surfaces and (b and d) the graphene paper surfaces.

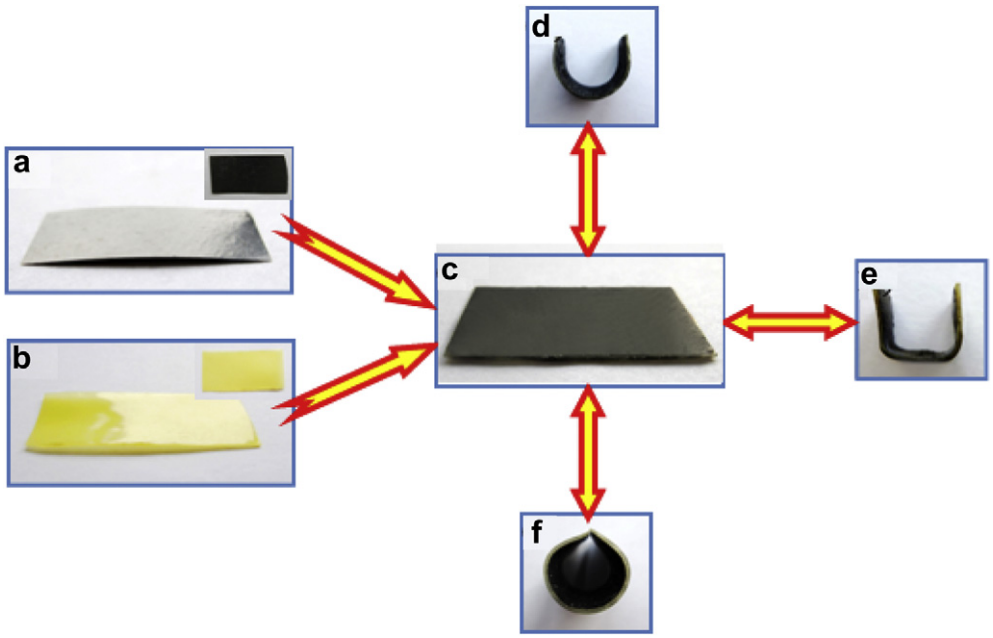

Fig. 6. Digital camera images of the samples: (a) the initial graphene paper, (b) initial pure PU film, the as-prepared graphene/PU composite film with U-shape (d), groove-shape (e) and O-shape (f). These shapes can be formed at 80 °C and fixed at room temperature. When the temperature is arrived at 80 °C once more, the graphene/PU composite film with the fixed shapes recovers instantly to the original shape.

1730 cm^{-1} and 1703 cm^{-1} are the free and hydrogen bonded carbonyl C═O stretch of urethane, respectively [34,35].

Fig. 4(a) shows a whole free-standing graphene paper, which was formed on a membrane filter by flow-directed assemble and then peeled off from the membrane. The paper is bendable and electrically conductive. As many papers reported, graphene paper displays excellent mechanical and electrical properties that make it potentially suitable for power supply device and structural composite applications [10]. Fig. 4(b) shows the top view of the graphene paper after being bonded on the PU film. The graphene paper still exhibits a shiny metallic luster on the surface and keeps the good conductivity of the pristine-graphene paper.

As shown in Fig. 5, layered structure of graphene paper is clearly identified based on the cross-sectional SEM images. The interface between graphene paper and PU matrix can be acquired and there is no obvious space cavity on the interface, indicating that the graphene paper is fixed strongly on the PU matrix. In addition, SEM analysis further reveals that the surface of the graphene paper is quite smooth. The reason can be attributed to the use of layer-by-layer (LBL) flow-directed assembly which can built up complex and controllable graphene-based nanosystems [36,37]. Based on the sp^2 state of GNS, LBL assembled graphene paper has high conductivity, because separate conjugated systems become interconnected to form a conducting network [38].

Fig. 6 shows the preparation procedure of the graphene/PU composite film with different shapes. In our synthesis, the DMF was used as a binder to bond both graphene paper and PU film. After being dried in the vacuum at 80 °C, the resulting graphene/PU composite film shows the excellent shape holding capacity. The flat graphene/PU composite film can be bent into different shapes at 80 °C, such as U-shape (d), groove-shape (e) and O-shape (f), and these shapes can be fixed after cooling down to room temperature.

Also, the graphene/PU composite film shows excellent shape recovery ability. While the temperature reaches 80 °C again, the fixed shape recovers instantly (see Supplementary data). As shown in Fig. 7, this recovery process is very rapid and the whole process is less than 1 s. After recovery, the graphene/PU composite film still can keep its original shape, which would be benefit for the repeating figuration of the different shaped composite films. This recovery is attributed to the fact that the shape-memory effect of segmented polyurethane block copolymers (PCL/PU) resulting from the phase-separated structure of its hard (isocyanate and 1,4-butyl glycol) and soft (PCL) segments [37]. Here, the graphene paper does not affect the recovery capacity of PU phase based on the good flexibility of graphene paper. It can be seen that graphene paper is still integrated, showing that the integrity of graphene layer is still kept after recovery. Also, the graphene paper is a functional material, which does not only act as a conducting agent, but also as a current collector [16]. The graphene/PU composite film can be directly used to fabricate a supercapacitor electrode, which doesn't need the insulating binder or the conducting additive. Therefore,

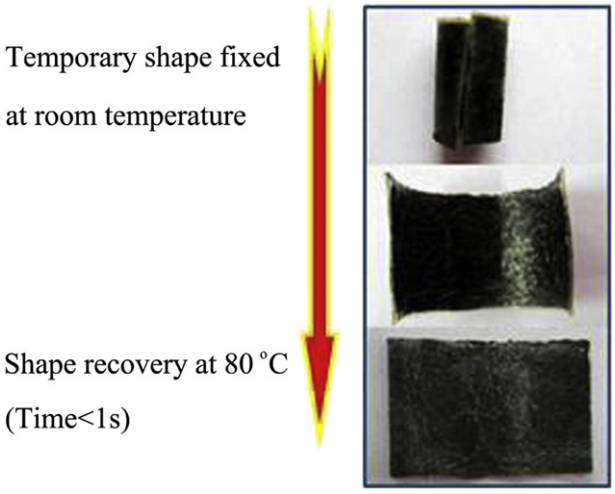

Fig. 7. Recovery process of the graphene/PU composite film from a rolled-up O-shape to a fully spreaded rectangle (20 mm × 10 mm × 3 mm) at 80 °C.

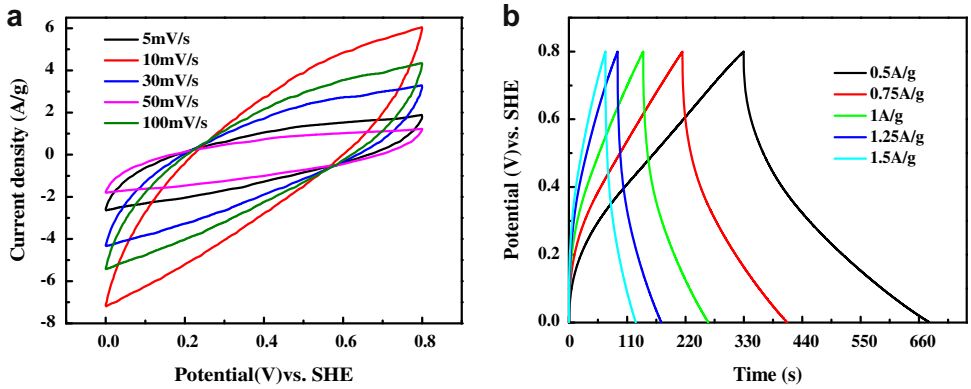

Fig. 8. Electrochemical properties of the graphene/PU composite film in 1 M H_2SO_4 medium in a three-electrode system. (a) CV curves at different sweep rates. (b) The charge/discharge curves at different current densities.

the graphene/PU composite film is expected that it not only has good electrochemical capacitive performance, but also has good shape-memory abilities.

Supplementary data related to this article can be found online at doi:10.1016/j.powsour.2012.03.086.

Fig. 8(a) shows the CV curves of the graphene/PU composite film electrode at different sweep rates between 0 and 0.8 V (vs. SCE) in 1 M H_2SO_4 aqueous electrolyte. At the sweep rates of 5 mV s^{-1} and 10 mV s^{-1}, the CV curves are nearly rectangular in shape without obvious redox peaks, indicating that the graphene/PU composite film has a double-layer electric capacitive behavior. As the sweep rate further increases, the CV curves deviate from the rectangular shape. It may be caused by the high resistivity compared with the metal collector [39]. Fig. 8(b) shows the galvanostatic discharge curves of the graphene/PU composite film electrode at different current densities. According to the capacitance equation, the specific capacitances of graphene/PU composite electrode at different current densities of 0.5 A g^{-1}, 0.75 A g^{-1}, 1 A g^{-1}, 1.25 A g^{-1} and 1.5 A g^{-1} are 218 F g^{-1}, 187 F g^{-1}, 156 F g^{-1}, 130 F g^{-1} and 110 F g^{-1}, respectively. As the discharge current increases, a large voltage drop is produced, and finally the capacitance decreases. This phenomenon may be explained by referring to the OH^- ion diffusion processes during the charging/discharging for the electrode. At high sweep rates with high current density significant OH^- ions are required to intercalate swiftly at the interface of electrode/electrolyte, however, the relatively low concentration of OH^- ions can't meet this demand and the processes would be controlled by the ion diffusion [40].

Stoller et al. fabricated a symmetric supercapacitor based on chemically reduced GO to give a specific capacitance of 135 F g^{-1} in KOH electrolyte [41]. Le et al. fabricated a supercapacitor using thermal-reduced GO, which has a specific capacitance of 132 F g^{-1} in 1 M H_2SO_4 electrolyte [42]. Here, the graphene paper bonded on PU film shows a satisfactory capacitance of graphene material, indicating that the promising specific capacitance of graphene/PU.

In fact, lots of reports have showed that graphene sheets display excellent capacitive properties, which can be comparable with conventional activated carbons (ACs) [43]. Moreover, graphene sheets even show faster charge-rate compared with ACs [44]. It is mainly due to the better electrical conductivity and the unique 2-dimentional planer structure compared with ACs [45,46]. Secondly, as reported by R.R. Nair et al., there are a lot of empty spaces formed between nonoxidized regions of graphene sheets. These empty spaces form a network of pristine-graphene capillaries within graphene paper [47]. After immersing the graphene paper into an electrolyte, the electrolyte molecules can be percolated into the graphene paper by a network of pristine-graphene capillaries. The complete contact between graphene sheets and electrolyte molecules would provide the capacitance of graphene papers. Therefore, the graphene paper still has the good capacitance.

EIS analysis is recognized as one of the principal methods examining the fundamental behavior of electrode materials for supercapacitors. For further understanding, impedance of the graphene/PU composite film was measured in the frequency range of 10 kHz to 0.1 Hz at open circuit potential with an AC perturbation of 5 mV. As shown in Fig. 9, the impedance spectrum is almost no appearance of an arc at a higher frequency region but with a spike at a lower frequency region, which indicates that the electron transfer resistance of the graphene/PU film is very low due to the excellent conductivity of graphene providing the efficient electron transfer channels [7]. The line at the low frequency region makes a 45° angle with the real axis, the Warburg line, and is a result of the frequency dependence of ion diffusion at the

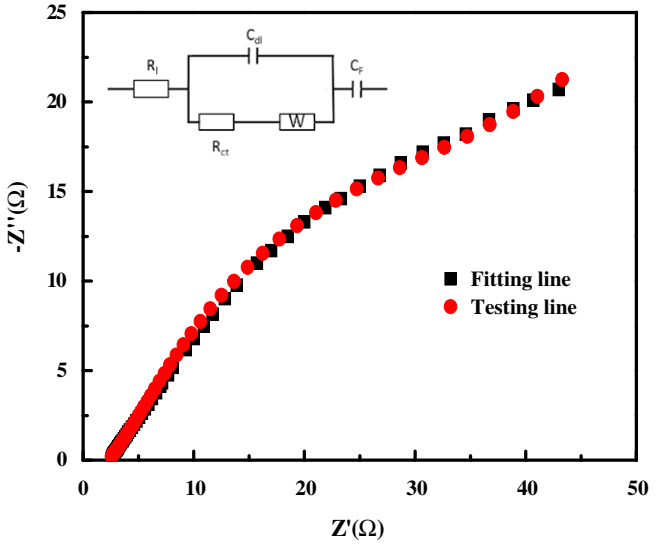

Fig. 9. Complex-plane impedance plots of the graphene/PU electrode. The inset is the equivalent circuit.

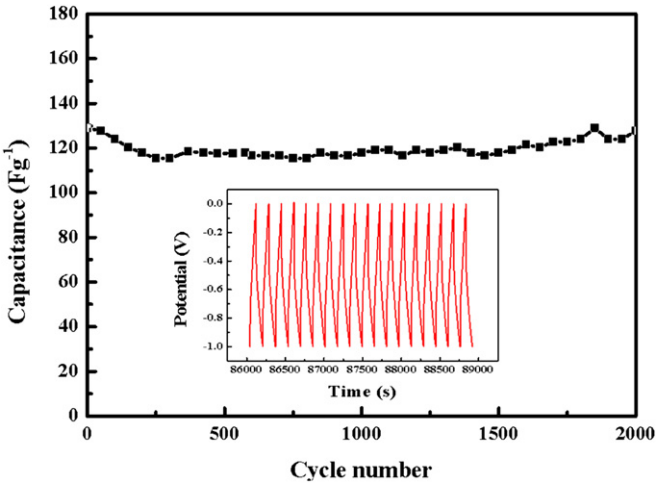

Fig. 10. Cycle life of the graphene/PU composite film electrode at the current density of 0.75 A g^{-1}. The inset is charge/discharge curves of the graphene/PU composite film electrode.

electrolyte/electrode interface. And the phase angle for impedance plot of the electrode was observed to be about 45° at low frequencies, implying the electrode was partly controlled by diffusion process [41].

Moreover, it can be seen that the simulation curve is almost completely coincidence with the original curve, implying the equivalent circuit in the inset of Fig. 9 is better to depict the electrochemical process at the electrode/electrolyte interface. It is composed of five elements: the internal resistance (RL), including the bulk electrolyte solution resistance, the intrinsic resistance of active material, and the electron transfer resistance at current collector/electrode boundary; the electrical double-layer capacitance (Cdl); the charge transfer resistance (Rct); the Warburg impedance (ZW); and the pseudo-capacitance (CF).

In order to evaluate the cycling stability of the graphene/PU composite film electrode, galvanostatic charge/discharge studies were performed at a constant current density of 1 A g^{-1} between 0 V and 0.8 V in 1 M H_2SO_4 electrolyte. The long-cycle performance is shown in Fig. 10, and the typical charge/discharge curves are shown as an inset. After 2000 cycles, the specific capacitance of the graphene/PU electrode remains 95% (148 F g^{-1}) of the initial capacitance. This suggests that the graphene/PU film possesses the good cycling stability. It is mainly attributed to the good electrochemical double-layer performance and superior electron transportation properties of graphene [41,48]. Also, the special structure of LBL assembled graphene film provides the conductive channels to improve the electrochemical performance. On the other hand, the prominent stability should be ascribed to the good combination between the graphene layer and PU film, to obtain a stable bi-layer architecture.

4. Conclusion

In summary, we have prepared a novel supercapacitor electrode material, in which graphene paper is used as electrochemically active material and PU film is used as shape holding matrix. Based on the good flexibility of graphene paper and the outstanding shape holding capacity of PU phase, the bi-layered graphene/PU composite film can be made into different shapes Also, the composite film shows excellent shape recovery ability. Furthermore, the graphene/PU composite film shows outstanding electrochemical performances, such as high specific capacitance, low electron transfer resistance, and good stable cycle life. We believe that, the ideal combination between the advantages from graphene phase (excellent conductivity and good supercapacitive performance) and the advantages from PU phase (excellent shape holding capacity and shape recovery ability) would make it attractive for the next-generations of tunable electrode materials.

Acknowledgment

This work was supported by the Top Hundred Talents Program of Chinese Academy of Sciences and the National Nature Science Foundations of China (51005225).

References

[1] W.W. Liu, X.B. Yan, J.W. Lang, Q.J. Xue, J. Mater. Chem. 21 (2011) 13205–13212.
[2] J.W. Lang, L.B. Kong, W.J. Wu, Y.C. Luo, L. Kang, Chem. Commun. 35 (2008) 4213–4215.
[3] X.B. Yan, Z.X. Tai, J.T. Chen, Q.J. Xue, Nanoscale 3 (2011) 212–216.
[4] S.Q. Chen, Y. Wang, J. Mater. Chem. 20 (2010) 9735–9739.
[5] J.W. Lang, X.B. Yan, X.Y. Yuan, J. Yang, Q.J. Xue, J. Power Sources 196 (2011) 10472–10478.
[6] C.Z. Meng, C.H. Liu, L.Z. Chen, C.H. Hu, S.S. Fan, Nano Lett. 10 (2010) 4025–4031.
[7] B.J. Li, H.Q. Cao, J. Shao, G.Q. Li, M.Z. Qu, G. Yin, Inorg. Chem. 50 (2011) 1628–1632.
[8] X.B. Yan, J.T. Chen, J. Yang, Q.J. Xue, P. Miele, ACS Appl. Mater. Interfaces 2 (2010) 2521–2529.
[9] K.Y. Shin, J.Y. Hong, J. Jang, Adv. Mater. 23 (2011) 2113–2118.
[10] D.A. Dikin, S. Stankovich, E.J. Zimney, R.D. Piner, G.H.B. Dommett, G. Evmenenko, S.T. Nguyen, R.S. Ruoff, Nature 448 (2007) 457–460.
[11] C.M. Chen, Q.H. Yang, Y.G. Yang, W. Lv, Y.F. Wen, P.X. Hou, M.Z. Wang, H.M. Cheng, Adv. Mater. 21 (2009) 1–5.
[12] Y.X. Xu, Q. Wu, Y.Q. Sun, H. Bai, G.Q. Shi, ACS Nano 4 (2010) 7358–7362.
[13] H.Q. Chen, M.B. Müller, K.J. Gilmore, G.G. Wallace, D. Li, Adv. Mater. 20 (2008) 3557–3561.
[14] J.K. Lee, K.B. Smith, C.M. Hayner, H.H. Kung, Chem. Commun. 46 (2010) 2025–2027.
[15] A. Abouimrane, O.C. Compton, K. Amine, S.T. Nguyen, J. Phys. Chem. C 114 (2010) 12800–12804.
[16] H. Gwon, H.S. Kim, K.U. Lee, D.H. Seo, Y.C. Park, Y.S. Lee, B.T. Ahna, K. Kang, Energ. Environ. Sci. 4 (2011) 1277–1283.
[17] Z.P. Li, Y.J. Mi, X.H. Liu, S. Liu, S.R. Yang, J.Q. Wang, J. Mater. Chem. 21 (2011) 14706–14711.
[18] Q. Wu, Y.X. Xu, Z.Y. Yao, A. Liu, G.Q. Shi, ACS Nano 4 (2010) 1963–1970.
[19] A.G. Pandolfo, A.F. Hollenkamp, J. Power Sources 157 (2006) 11–27.
[20] R. Mohr, K. Kratz, T. Weigel, M. Lucka-Gabor, M. Moneke, A. Lendlein, Proc. Natl. Acad. Sci. U.S.A. 103 (2006) 3540–3545.
[21] E. Rodriguez, X. Luo, P. T. Mather, Materials Research Society Fall Meeting, Boston, MA, 2008.
[22] J.H. Kim, T.J. Kang, W.R. Yu, Int. J. Plast. 26 (2010) 204–218.
[23] L. Nyholm, G. Nystrom, A. Mihranyan, M. Stromme, Adv. Mater. 23 (2011) 3751–3769.
[24] J.M. Tarascon, M. Armand, Nature 414 (2001) 359–367.
[25] J. Liu, H. Xia, D. Xue, L. Lu, J. Am. Chem. Soc. 131 (2009) 12086–12087.
[26] H. Nishide, K. Oyaizu, Science 319 (2008) 737–738.
[27] J.A. Rogers, T. Someya, Y.G. Huang, Science 327 (2010) 1603–1607.
[28] V.L. Pushparaj, M.M. Shaijumon, A. Kumar, S. Murugesan, L.C.R. Vajtai, R.J. Linhardt, O. Nalamasu, P.M. Ajayan, Proc. Natl. Acad. Sci. U.S.A. 104 (2007) 13574–13577.
[29] L. Hua, J.W. Choi, Y. Yang, S. Jeong, F.L. Mantia, L.F. Cui, Y. Cui, Proc. Natl. Acad. Sci. U.S.A. 106 (2009) 21490–21494.
[30] Y.X. Xu, H. Bai, G. Lu, W.C. Li, G.Q. Shi, J. Am. Chem. Soc. 130 (2008) 5856–5857.
[31] W.,S. Hummers, R.E. Offeman, J. Am. Chem. Soc. 80 (1958) 1339.
[32] Z.X. Tai, H.B. Ma, B. Liu, X.B. Yan, Q.J. Xue, Colloids Surf., B 89 (2012) 147–151.
[33] D. Li, M.B. Müller, S. Gilje, R.B. Kaner, G.G. Wallace, Nat. Nanotechnol. 3 (2008) 101–105.
[34] A. Mishra, V.K. Aswal, P. Maiti, J. Phys. Chem. B 114 (2010) 5292–5300.
[35] W. Wang, Y. Jin, Z.H. Su, J. Phys. Chem. B 113 (2009) 15742–15746.
[36] P.T. Hammond, Adv. Mater. 16 (2004) 1271–1293.
[37] M.K. Gheith, T.C. Pappas, A.V. Liopo, V.A. Sinani, B.S. Shim, M. Motamedi, J.P. Wicksted, N.A. Kotov, Adv. Mater. 18 (2007) 3203–3224.
[38] C.A. Leon, L.R. Radovic, Chemistry and Physics of Carbon, vol. 4, Marcel Dekker, New York, 1994, p. 213.
[39] E. Frackowiak, F. Beguin, Carbon 39 (2001) 937–950.
[40] J.W. Lang, L.B. Kong, W.J. Wu, M. Liu, Y.C. Luo, L. Kang, J Solid State Electrochem. 13 (2009) 333–340.

[41] M.D. Stoller, S. Park, Y. Zhu, J. An, R.S. Ruoff, Nano Lett. 8 (2008) 3498–3502.
[42] L.T. Le, M.H. Ervin, H. Qiu, B.E. Fuchs, W.Y. Lee, Electrochem. Commun. 13 (2011) 355–358.
[43] Z.D. Huang, B. Zhang, S.W. Oh, Q.B. Zheng, X.Y. Lin, N. Yousefi, J.K. Kim, J. Mater. Chem. 22 (2012) 3591–3599.
[44] J.R. Miller, R.A. Outlaw, B.C. Holloway, Science 329 (2010) 1637–1639.
[45] C. Vallés, J.D. Núñez, A.M. Benito, W.K. Maser, Carbon 50 (2012) 835–844.
[46] W.T. Deng, X.B. Ji, M. Gómez-Mingot, F. Lu, Q.Y. Chen, C.E. Banks, Chem. Commun. 48 (2012) 2770–2772.
[47] R. KÖtz, M. Carlen, Electrochim. Acta 45 (2000) 2483–2498.
[48] C.H. Xu, J. Sun, L. Gao, J. Mater. Chem. 21 (2011) 11253–11258.